

# **Supplementary Information**

## **Atomic MoS<sub>2</sub> Monolayers Synthesized from Metal-Organic Complex by Chemical Vapor Deposition**

Lina Liu <sup>a†</sup>, Hailong Qiu <sup>a,b†</sup>, Jingyi Wang <sup>a</sup>, Guanchen Xu <sup>a</sup> and Liying Jiao <sup>a\*</sup>

- 1. Experimental Details**
- 2. More characterizations on Mo-DMDTC**
- 3. Thermal decomposition of Mo-DMDTC**
- 4. More characterizations on as-grown MoS<sub>2</sub>**
- 5. Effects of growth temperature and substrate**
- 6. Promotion effect of Mo-DMDTC ligand**
- 7. AES measurements on the transferred MoS<sub>2</sub> flakes**
- 8. More electrical data on MoS<sub>2</sub> devices**
- 9. Comparison of MoS<sub>2</sub> grown with different approaches**

# 1. Experimental Details

## (1) Synthesis of Mo-DMDTC

Molybdenum dimethyldithiocarbamate complex (Mo-DMDTC) was synthesized by the coprecipitation between  $\text{MoCl}_5$  (Alfa Aesar, 99.6%) and sodium dimethyldithiocarbamate (Na-DMDTC) (Sigma Aldrich, 98%) in aqueous solution. A solution of Na-DMDTC (6 mmol in 10 mL DI water) was added to the aqueous solution of  $\text{MoCl}_5$  (1 mmol in 80 mL DI water) under magnetic stirring for 6 h at room temperature. Dropwise addition of Na-DMDTC solution resulted in purple-colored precipitate (Mo-DMDTC), which was separated by centrifuging at 5,000 rpm for 10 min and dried at  $\sim 70^\circ\text{C}$  in air.

## (2) Growth of monolayer $\text{MoS}_2$ flakes

The growth of monolayer  $\text{MoS}_2$  flakes was carried out in a home-built CVD furnace with 1 inch quartz tube under atmospheric pressure (Figure S1). Mo-DMDTC ( $40\ \mu\text{L}$ ,  $4\ \text{mg}\cdot\text{mL}^{-1}$  dispersed in ethanol) was drop-dried onto a sapphire substrate and placed in the center of the furnace. Another sapphire substrate with a size of  $\sim 3\ \text{cm}\times 1.5\ \text{cm}$  covered on the substrate supporting Mo-DMDTC (facing down as grown substrate). Sulfur powder was placed in a ceramic boat upstream. After purging the system with Ar for 5 min, the furnace was heated up to  $650^\circ\text{C}$  in 12 min with 150 sccm Ar. When the temperature of furnace reached  $650^\circ\text{C}$ , sulfur was heated by a heating belt at  $\sim 170^\circ\text{C}$ . After 40 min, the furnace was heated up to  $800^\circ\text{C}$  and stayed at this temperature for 10 min. Then the furnace was naturally cooled down to room temperature and the heating belt was removed at  $\sim 400^\circ\text{C}$ .

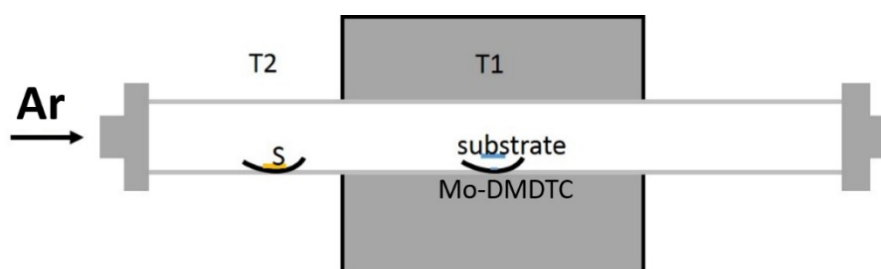


**Figure S1** Schematic for the set-up used for the growth of  $\text{MoS}_2$  flakes

## (3) Transfer of $\text{MoS}_2$ flakes

After the growth, the sapphire substrate with  $\text{MoS}_2$  flakes was coated with PMMA thin film (Allresist GmbH, AR-P 679.04) by spin-coating at 2,000 rpm for 1 min, followed by baking at  $170^\circ\text{C}$ .

°C for 2 h. Then the baked sample was soaked in hot KOH solution (5 wt %). After the PMMA film detached from the substrate, the PMMA film was taken out of the KOH solution and rinsed thoroughly with DI water. The cleaned PMMA film was attached to a 300 nm thick SiO<sub>2</sub>/Si substrate and baked at ~80 °C to promote the interaction of MoS<sub>2</sub> flakes with the substrate. Finally, the PMMA film was removed by acetone vapor to leave MoS<sub>2</sub> flakes on the substrate.

#### (4) Device fabrication and measurement

Source and drain electrodes (10 nm Ti/50 nm Au) were fabricated on MoS<sub>2</sub> flakes by electron-beam lithography followed by electron-beam evaporation on 300 nm SiO<sub>2</sub>/Si substrates. The channel length of FETs we made was ~1.0 μm. The obtained MoS<sub>2</sub> FETs were measured with probe station in vacuum at a base pressure of ~10<sup>-5</sup> mbar at room temperature using Agilent B1500A. The mobility of FETs was estimated using the method according to previous report<sup>1</sup>.

#### (5) Characterizations

The FTIR spectra were collected with Bruker VERTEX 70 and the UV-vis spectra were taken with Hitachi Limited U-3900. XPS and TG-MS curves were taken with Thermo Scientific Escalab 250Xi and NETZSCH X70, respectively. AES was collected with ULVAC-PHI 700. TOF-SIMS was taken with TOF.SIMS 5. The optical images were taken with Olympus BX 51M microscope. AFM images were captured with Bruker Dimension Icon in scanasyst mode. Raman and PL spectra were collected with Horiba-Jobin-Yvon Raman system using a 514 nm laser. TEM images, SAED patterns and high resolution TEM images were taken with JEOL 2100 at 200 KV.

## 2. More characterizations on Mo-DMDTC

According to the TG-MS analysis, the thermal-decomposition of Mo-DMDTC displayed a two-step weight loss and four major products were detected during the decomposition process (Figure S2(b), (c) and (d)). The existence of H<sub>2</sub>O (*m/z* = 18) indicated that hydrated water was contained in Mo-DMDTC. The other two products were assigned to CO (*m/z* = 28) and CO<sub>2</sub> (*m/z* = 44) which could be possibly attributed to the mild oxidation of some organic products by trace oxygen in the system. The product with a *m/z* of 76 should be CS<sub>2</sub>. Due to the limitation of this test, only gas with boiling point lower than 200 °C could be detected. We can infer that the DMDTC ligand should mainly change to CS<sub>2</sub> and (CH<sub>3</sub>)<sub>2</sub>NCSN(CH<sub>3</sub>)<sub>2</sub> based on previous studies

on the thermal-decomposition of other metal-DMDTC complexes<sup>2</sup>.

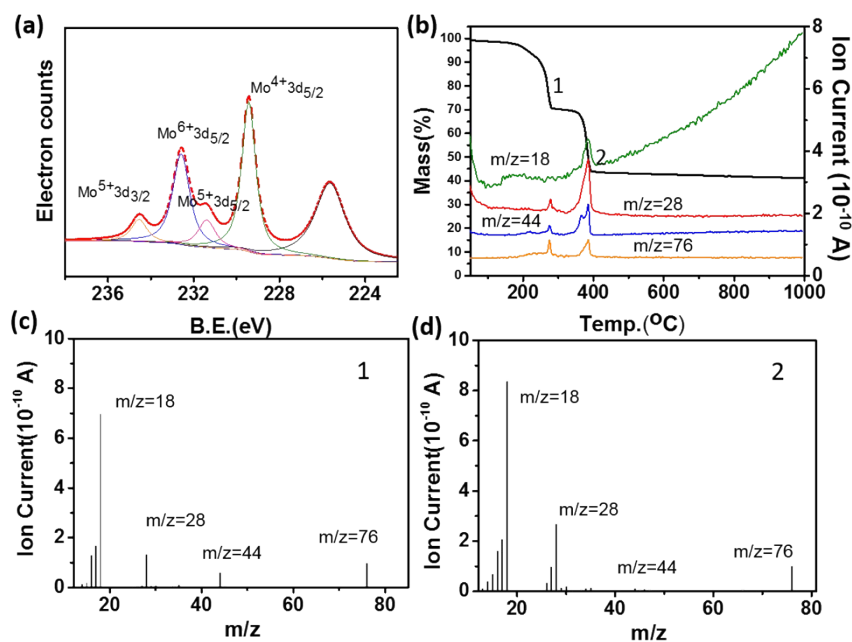


**Figure S2** (a) XPS of Mo-DMDTC. (b) TG curve and MS ion currents of characteristic fragments for the decomposition of Mo-DMDTC. (c, d) Two typical mass spectra for the products produced at the steps marked with 1 and 2 in (b), respectively.

### 3. Thermal decomposition of Mo-DMDTC

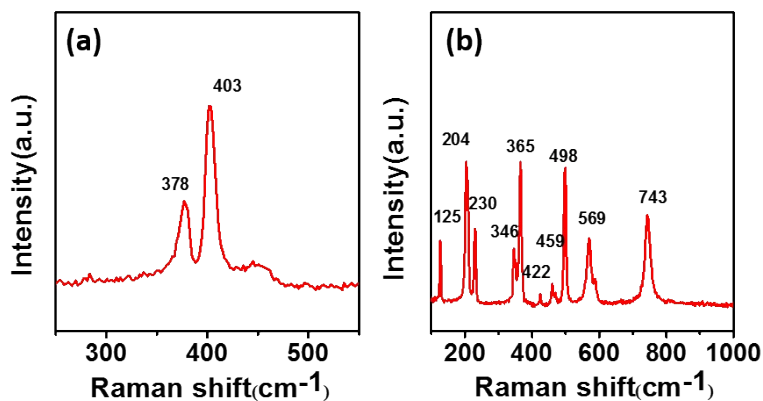


**Figure S3** Raman measurements on the thermal decomposition products of Mo-DMDTC. (a) Raman spectroscopy of Mo-DMDTC after TG test. (b) Raman spectroscopy of the remained materials of Mo-DMDTC that deposited on the substrate after annealing at 400 °C in our CVD system.

## 4. More characterizations on as-grown MoS<sub>2</sub>

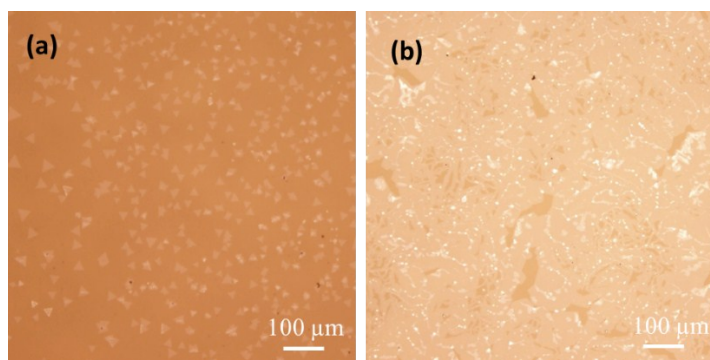


**Figure S4** Low magnification optical images of typical growth results. (a) Individual MoS<sub>2</sub> flakes. (b) Continuous MoS<sub>2</sub> film.

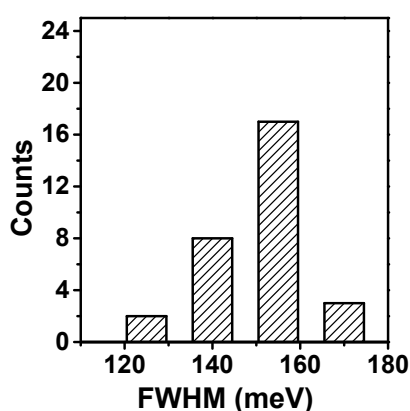


**Figure S5** The distribution of A-exciton PL peak FWHM in 30 MoS<sub>2</sub> flakes

## 5. Effects of growth temperature and substrate

The optimized growth temperature for MoS<sub>2</sub> was 800 °C. At a lower growth temperature of 600 °C, only small MoS<sub>2</sub> pieces could be found on the growth substrate (Figure S6b). At a higher growth temperature of 900 °C, the obtained MoS<sub>2</sub> flakes were larger in size (~60 μm) but the edges were not straight and multiple layers were grown on the top of the 1L flakes (Figure S6d). Besides sapphire, the growth of MoS<sub>2</sub> can also be achieved on SiO<sub>2</sub>/Si substrates, but the shape of the obtained flakes is not as regular as those grown on sapphire substrates (Figure S7).

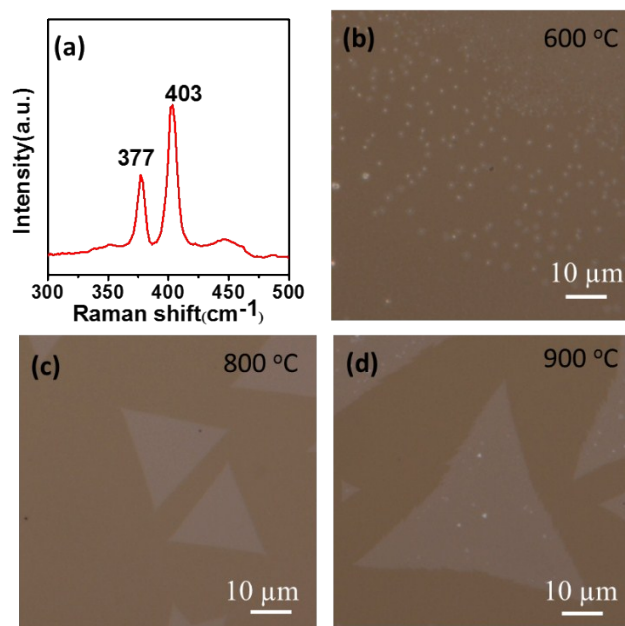


**Figure S6** (a) Raman spectrum of the remained materials after the TGA tests. (b, c, d) MoS<sub>2</sub> flakes grown at different temperatures.

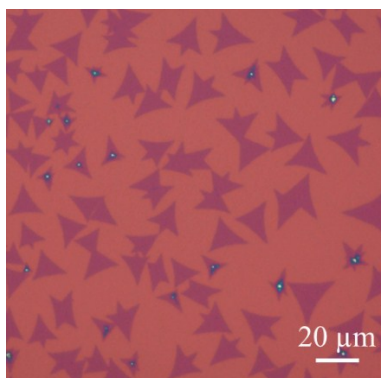


**Figure S7** MoS<sub>2</sub> flakes grown on SiO<sub>2</sub>/Si substrate

## 6. Promotion effect of Mo-DMDTC ligand

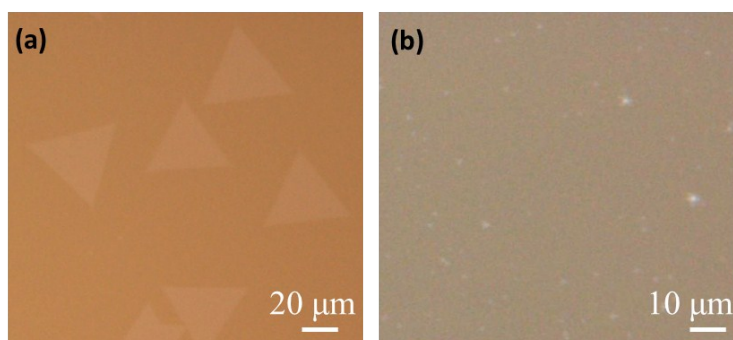


**Figure S8** (a) Typical growth result using Mo-DMDTC as precursor. (b) MoS<sub>2</sub> particles grown from Mo-DMDTC after the removal of organic ligands by heating at 1000 °C in Ar.

## 7. AES measurement on the transferred MoS<sub>2</sub> flakes

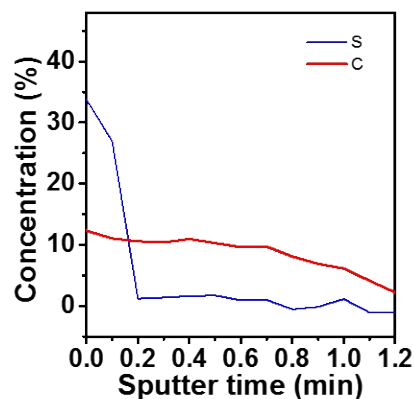


**Figure S9** Depth profiling analysis of S and C atomic concentrations on the transferred MoS<sub>2</sub> flakes with Auger electron spectroscopy (AES).

## 8. More electrical data on MoS<sub>2</sub> devices

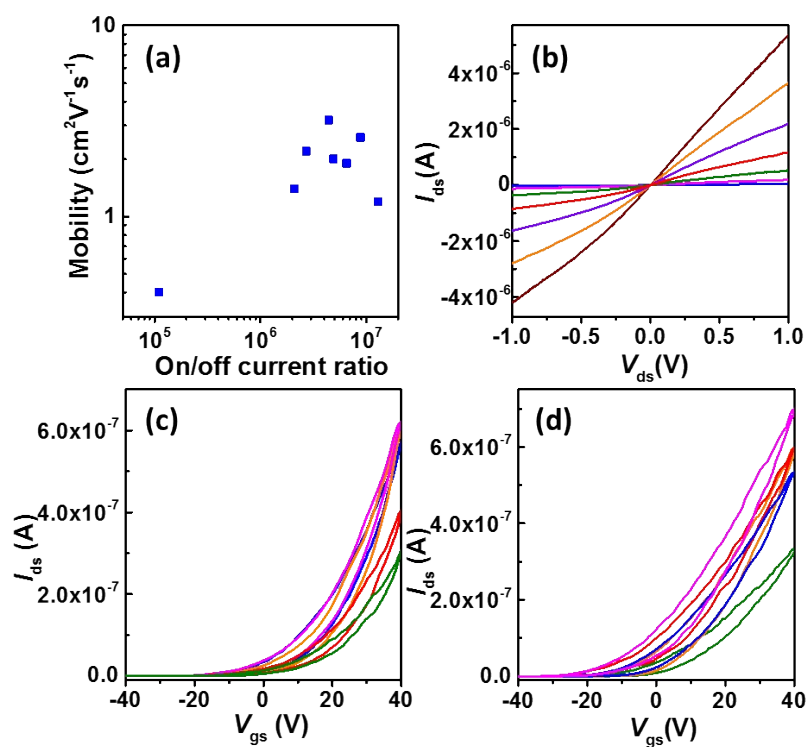


**Figure S10** (a) The distribution of mobility and on/off current ratios of 8 MoS<sub>2</sub> FETs. (b)  $I_{ds}$ - $V_{ds}$  curves for the device in Figure 5(a) at varied  $V_{gs}$  from -40 to 40 V at steps of 10 V from bottom to top. (c, d) Hysteresis in  $I_{ds}$ - $V_{gs}$  curves for ten FETs made on MoS<sub>2</sub> flakes grown with Mo-DMDTC and MoO<sub>3</sub> (five devices for each type) at  $V_{ds}$ =0.5 V, respectively.

## 9. Comparison of MoS<sub>2</sub> grown with different approaches

The comparison on grain size and mobility between our MoS<sub>2</sub> flakes and several previous results were listed in the following table. The grain size and mobility of our flakes showed a reasonable value among the existing results with similar device configurations.

**Table S1** Comparison of 1 L MoS<sub>2</sub> flakes grown with different approaches

CVD MoS <sub>2</sub>	Grain size	Mobility (cm <sup>2</sup> V <sup>-1</sup> s <sup>-1</sup> )
This work	20-30 μm	1.2-3.2
Y. H. Lee. et al. <i>Adv. Mater.</i> , 2012, <b>24</b> , 2320-2325.	~160 nm	0.02
X. Wang. et al. <i>J Am. Chem. Soc.</i> , 2013, <b>135</b> , 5304-5307.	~10 μm	0.1-0.7
Najmaei, S. et al. <i>Nano Lett.</i> 2014, <b>14</b> , 1354-1361.	~20 μm	1.9
Q. Zhang. et al. <i>Angew. Chem. Int. Ed.</i> , 2015, <b>54</b> , 8957-8960	20-40 μm	~ 6

**Note:** The FETs in the table were all fabricated with CVD grown MoS<sub>2</sub> flakes transferred onto SiO<sub>2</sub>/Si substrate with similar device configuration and similar post-fabricated thermal treatments.

## References

1. B. Radisavljevic, A. Radenovic, J. Brivio, V. Giacometti and A. Kis, *Nat. Nanotechnol.*, 2011, **6**, 147-150.
2. C. G. Sceney, J. F. Smith, J. O. Hill and R. J. Magee, *J. Therm. Anal.*, 1976, **9**, 415-423.
3. Y. H. Lee, X. Q. Zhang, W. Zhang, M. T. Chang, C. T. Lin, K. D. Chang, Y. C. Yu, J. T. Wang, C. S. Chang, L. J. Li and T. W. Lin, *Adv. Mater.*, 2012, **24**, 2320-2325.
4. X. Wang, H. Feng, Y. Wu and L. Jiao, *J Am. Chem. Soc.*, 2013, **135**, 5304-5307.
5. Najmaei, S.; Zou, X.; Er, D.; Li, J.; Jin, Z.; Gao, W.; Zhang, Q.; Park, S.; Ge, L.; Lei, S.; Kono, J.; Shenoy, V. B.; Yakobson, B. I.; George, A.; Ajayan, P. M.; Lou, J. *Nano Lett.* **2014**, *14*, 1354-1361.
6. Q. Zhang, X. Xiao, R. Zhao, D. Lv, G. Xu, Z. Lu, L. Sun, S. Lin, X. Gao, J. Zhou, C. Jin, F. Ding and L. Jiao, *Angew. Chem. Int. Ed.*, 2015, **54**, 8957-8960.